

---

This is an electronic reprint of the original article.  
This reprint may differ from the original in pagination and typographic detail.

Zhao, Weixin; Lestinen, Sami; Kilpelainen, Simo; Kosonen, Risto

## **An experimental study of the influence of a moving person on airflow characteristics and thermal conditions with diffuse ceiling ventilation**

*Published in:*  
Indoor and Built Environment

*DOI:*  
[10.1177/1420326X20917202](https://doi.org/10.1177/1420326X20917202)

Published: 01/07/2020

*Document Version*  
Publisher's PDF, also known as Version of record

*Published under the following license:*  
CC BY

*Please cite the original version:*  
Zhao, W., Lestinen, S., Kilpelainen, S., & Kosonen, R. (2020). An experimental study of the influence of a moving person on airflow characteristics and thermal conditions with diffuse ceiling ventilation. *Indoor and Built Environment*, 29(6), 860-880. Article ARTN 1420326X20917202. <https://doi.org/10.1177/1420326X20917202>

---

This material is protected by copyright and other intellectual property rights, and duplication or sale of all or part of any of the repository collections is not permitted, except that material may be duplicated by you for your research use or educational purposes in electronic or print form. You must obtain permission for any other use. Electronic or print copies may not be offered, whether for sale or otherwise to anyone who is not an authorised user.



# An experimental study of the influence of a moving person on airflow characteristics and thermal conditions with diffuse ceiling ventilation

Weixin Zhao<sup>1</sup> , Sami Lestinen<sup>1</sup> , Simo Kilpeläinen<sup>1</sup> and Risto Kosonen<sup>1,2</sup>

## Abstract

The influence of occupants' movements should be considered when analysing local thermal comfort. This study presents the effect of human movement on airflow characteristics and local thermal conditions with diffuse ceiling ventilation by experimental studies. A simulated person moving was used to study the human movement in an office. In these experiments, three moving speeds were studied: 0.3, 0.6 and 1.0 m/s. The simulated person moved in four cycle patterns: continuous moving and with 5 s, 10 s and 15 s interval breaks between each turn. Three heat gain levels of 40, 60 and 80 W/m<sup>2</sup> were evaluated in the chamber. The results indicate that the human movement decreased vertical temperature gradient compared with the steady-state condition. Instead, the moving intervals would have no effect on the vertical air temperature gradient. The power spectral density was increased by 90% due to the person movement compared with the steady-state condition. The moving person would create different micro-environments close to work stations than close to the moving area.

## Keywords

Diffuse ceiling ventilation, Local thermal comfort, Moving person, Airflow characteristics, Induced airflow

Accepted: 14 March 2020

## Introduction

In modern cities and urban societies, the influence of indoor environment to human health, comfort and productivity is important<sup>1,2</sup> because people spend more than 90% of their time indoors.<sup>3</sup> Occupants expect to have healthy and comfortable indoor environment that could fulfil their need for thermal comfort as well as excellent indoor air quality. These conditions can be achieved by high-performance ventilation.

Diffuse ceiling ventilation (DCV) is a ventilation concept in which the suspended ceiling serves as an air diffuser to supply outdoor air into the room, where the air movement is dominated often by

buoyancy flows from heat sources and not by momentum flow from the supply. The supply air of DCV is distributed evenly through the perforated suspended ceiling down to the occupied zone. Diffuse ceiling air supply can create good thermal environment in heating

<sup>1</sup>Department of Mechanical Engineering, Aalto University, Espoo, Finland

<sup>2</sup>College of Urban Construction, Nanjing Tech University, Nanjing, China

## Corresponding author:

Weixin Zhao, Department of Mechanical Engineering, Aalto University, Espoo, Finland.

Email: weixin.zhao@aalto.fi

season. However, it will require higher energy consumption.<sup>4</sup>

Earlier studies have shown that large-scale circulating flow pattern exists with asymmetric thermal load distribution with diffuse ceiling ventilation increasing a vertical temperature gradient (about 1°C) at the whole space.<sup>5–8</sup> The effect of heat gain on indoor airflow characteristics was studied.<sup>8,9</sup> The result shows that the mean air speed and the airflow fluctuation were increased with heat gain and supply airflow rate. Consequently, also the turbulent kinetic energy and the turbulence dissipation would be increased. The results indicate a cause–effect relationship of the heat gain strength and the heat gain distribution on airflow characteristics that may also have effects on air distribution. Also, the air distribution of diffuse ceiling is affected by natural convection flows and asymmetrical heat gains arrangement, which may cause circulation and high velocities in the opposite side of heat sources.<sup>10</sup>

Together with the effect of heat gains on air movement, the influence of occupants' movements should also be considered. Previous studies indicated that the human movement in indoor environment has an influence on the dynamic airflow.<sup>11–14</sup> An upward air vortex and a strong downward airflow were found behind the moving body at different moving speeds. Also, a symmetric downward air flow along the vertical centreline of the moving body was observed.<sup>15</sup>

Mattsson<sup>16</sup> reported measurements from a full-scale displacement ventilated room where a heated dummy (1.63 m high cylinder) was located on a trolley. If the dummy without thermal load was doing a single motion, horizontal air movements would be created without mechanical ventilation. If the dummy was moved back and forth on a straight line by a conveyor belt, systematic periodical air movement would be recognized. The local field as well as the entire room airflow was found to be substantially influenced by occupants' movements. The air mixing is enhanced by increasing the speed of reciprocal movements of a person.<sup>17</sup>

Measurements and computational fluid dynamics (CFD simulations) of a displacement ventilated room with a cylinder type person simulator standing still and moving back and forth on a straight line were performed, respectively.<sup>18,19</sup> The speed varied between 0 and 1.0 m/s. Similar study was carried out by Feng.<sup>20</sup> The results showed that the vertical thermal stratification was disturbed and the local mean age of air decreased as the speed of the moving dummy increased. With displacement ventilation, a moving manikin could make the vertical temperature gradient smaller than in the steady-state conditions. Simultaneously, higher moving speed led to a smaller

local air exchange index in the occupied zone.<sup>21</sup> Halvoňová and Melikov<sup>22</sup> examined the effect of disturbances due to walking person with 'ductless' personalized ventilation in conjunction with displacement ventilation. The results revealed that the walking person disturbed the displacement principle and resulted in a decrease of the inhaled air quality. Yang and Sekhar<sup>23</sup> simulated the interaction of dynamic indoor environment with the moving person with a ceiling-mounted personalized ventilation system.

Some studies investigated the aerodynamic effect of human movement with different moving speeds and different frequency of limbs pendulum by experiment and numerical simulations without ventilation.<sup>24,25</sup> These studies show that the aerodynamic effect caused by human movements depend on the moving speed, moving distance and spatial location. The analysis results show that body motion has an influence on the flow field. Also, more detailed profile of the human body with movement would lead to more complicated flow field in the nearby area.

Previous studies also have found that the air distribution is affected by the moving person with mixing ventilation, stratum ventilation and displacement ventilation. The influence of the moving manikin on mixing ventilation was the smallest and the influence on stratum ventilation was smaller than on displacement ventilation. However, the disturbed room airflows would return to the original state quickly after the walking person remains motionless.<sup>26–28</sup>

In previous studies, different methods such as the small-scale test with positive input ventilation (PIV) experiment<sup>29</sup> and the simulation based on momentum theory<sup>30,31</sup> were introduced. Moreover, the transient airflow was studied with different spaces such as the operating room<sup>32</sup> and the subway.<sup>31</sup>

The literature shows that person movements have some impact on the airflow structure in the ventilated enclosures both in relation to the local field around a person as well as to the near zone of the occupant. No studies explored the effect of the moving person with different moving intervals on the airflow pattern and thermal comfort under diffuse ceiling ventilation. The extended predicted mean vote (ePMV) of the dynamic thermal comfort model was proposed to extend the PMV model to dynamic conditions.<sup>33</sup> In this study, the heat gain and the temperature are constant. The main focus was on local thermal comfort, and the draught rate and air velocity were selected as indices to analyse the thermal conditions with the moving person.

The novelty of this study is to analyse the effect of a moving person with different intervals on the performance of diffuse ceiling ventilation close to workstation with laboratory experiments. Also, the power

spectral density and fluctuation energy ratio were studied to analyse the effect of a moving person on the airflow structure close to workstations. The simulated moving person was designed to go back and forth on a straight line near workstations. The effect of the specific heat gain level and also moving speed and moving interval of the simulated person on the air flow pattern was studied. The selected measurement locations represent the micro-environment close to the workstation (P1) and moving zone (P2). The main objective was to analyse the effect of the moving person on the airflow characteristics and thermal conditions near the person and moving zone.

## Methods

Room air temperature, surface temperatures and air velocity were measured to evaluate thermal environment of studied cases. Local thermal comfort was analysed with draught rate. The power spectral density and fluctuation energy ratio were studied to observe the airflow fluctuation characteristics.

### Test room

The measurements were carried out in a test chamber of the internal dimensions of 5.5 m length, 3.8 m width and 3.2 m height from the floor up to the suspended ceiling. The supply air was distributed through the suspended ceiling panels into the room. The panels were installed 0.35 m below the ceiling. The diffuse ceiling panel has dimensions of  $600 \times 600 \times 20 \text{ mm}^3$ , and the panel was made of glass-wool-plate elements. Each tiny plastic nozzle has a diameter of 14 mm, and the overall perforation ratio is approximately 0.5% (Figure 1(a)). Two Ventiduct VSR duct diffusers<sup>34</sup> were installed sequentially above the suspended ceiling to be able to reach uniform static pressure over the ceiling panels. The combined duct diffuser of diameter 200 mm extended the entire length of the upper chamber (Figure 1(b)). The suspended ceiling was 50 mm below the duct. The exhaust grille was installed at floor (circle, length-coordinate 5 m, width-coordinate 2.4 m), as shown in Figure 2(a)). The diameter of the exhaust duct was 160 mm. The test chamber was located inside a laboratory hall such that the outer environment was stable.

### The experimental set-up

Figure 2 presents the layout of the test chamber. Two workstations were located in the middle of the room in longwise direction and 0.6 m from the window panel. Both workstations were equipped with a laptop and a monitor. Lights were installed in the middle of the workstation to the ceiling at a height of 3.2 m. The simulated solar heat gain was provided by hot-water

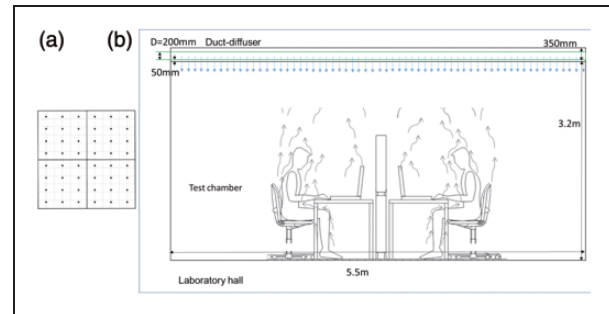


**Figure 1.** (a) Diffuse ceiling inlet structure with tiny nozzle density ( $d = 14 \text{ mm}$ ) of the entire panel ( $600 \times 600 \text{ mm}$ ) area and (b) duct diffuser ( $D = 200 \text{ mm}$ ) located in the plenum chamber over the ceiling panels.

pipes inside the window panel. The window panel surface was set to  $30\text{--}40^\circ\text{C}$  to simulate solar heat gain, as shown in Table 1. The insulation plates with a thickness of 0.1 m were installed outside the room to cover the window panel. The electric heating foil of 5 m length and 1 m width was installed on the floor 0.8 m from the heated window panel wall to simulate direct solar load, as shown in Figure 2(a)).

The use of real human movement makes the study more complicated, because to maintain the same walking speed and moving breaks for long time tests is difficult. Because of this reason, the Nordtest<sup>35</sup> was selected to simulate a moving person. According to Nordtest standard, the moving person is a plate with dimensions of 1.0 m height, 0.5 m width and the total height is 1.6 m from the floor. For the solidity and stability, a plate made by polyfoam with a 0.03 m thickness was used for the test to fulfil the demand of Nordtest. The moving person was fixed upon a trolley which a moving speed that was possible to control. The moving track was 3 m long and located 0.67 m from the wall in the longwise direction, as shown in Figure 3.

In this study, the occupied zone means the region normally occupied by people within a space, defined by ASHREA 55–2010.<sup>36</sup> The workstation zone is the area including desks and seated occupants, as shown in Figure 4. Because there are two measured locations, P1 (seated person zone) and P2 (moving zone), the seated person zone was named as the occupied zone accordingly.

### Experimental conditions

The average heat gain was designed at  $40 \text{ W/m}^2$ ,  $60 \text{ W/m}^2$  and  $80 \text{ W/m}^2$ . Table 1 shows the used heat gains in the test chamber. In this study, the supply temperature and exhaust temperature were constant with all heat gains. So when the heat gain rises (from  $40$  to  $80 \text{ W/m}^2$ ), a higher airflow rate is required to reach the same target room air temperature. In this study, the air flow rate was varied

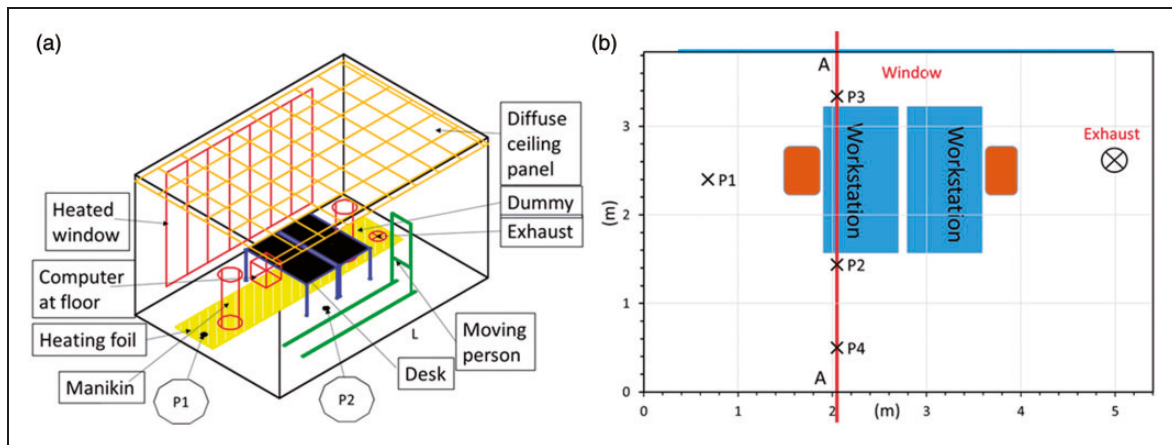


**Figure 2.** (a) The test chamber layout and the location of the moving simulated person and (b) measurement locations in the steady-state condition and the section A-A included the measurement locations of P2, P3 and P4. Note: Please refer to the online version of the article to view the figures in colour.

**Table 1.** Used heat gains in different test cases.

Total heat flux	Dummy	Manikin	Manikin equipment	Two laptops	Two monitors	Two lights	Window panel	Computer at floor	Solar load on the floor	Total heat gain
(W/m <sup>2</sup> )	(W)	(W)	(W)	(W)	(W)	(W)	(W)	(W)	(W)	(W)
40	75	83	67	75	78	116	346	0	0	840
60	75	83	67	75	78	116	346	0	420	1260
80	75	83	67	75	78	116	661	103	420	1678

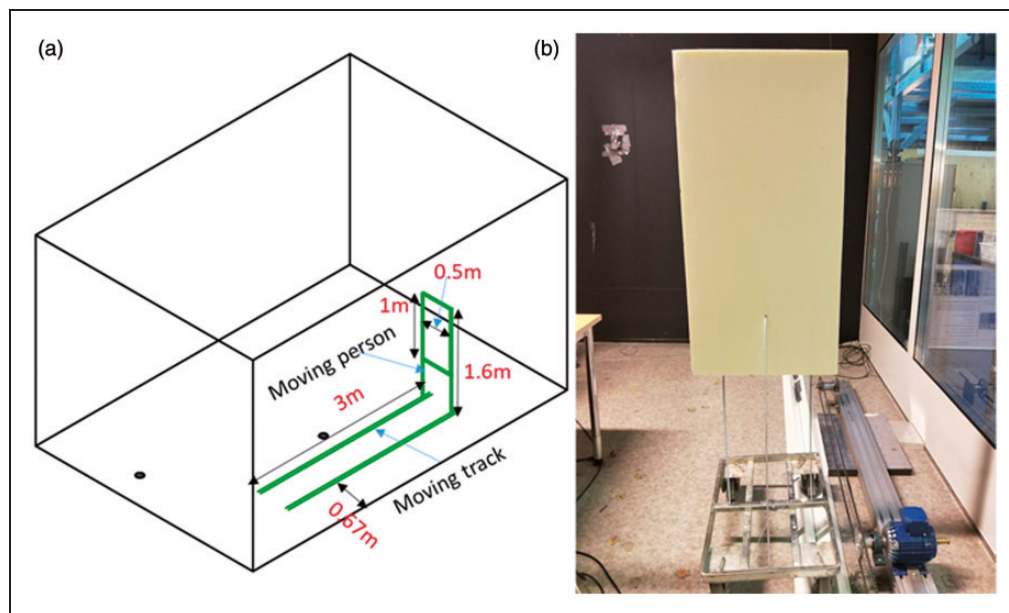


**Figure 3.** (a) A dimension of moving plate as a simulated moving person with trolley and moving track and (b) the simulated person moving on the track. Note: Please refer to the online version of the article to view the figures in colour.

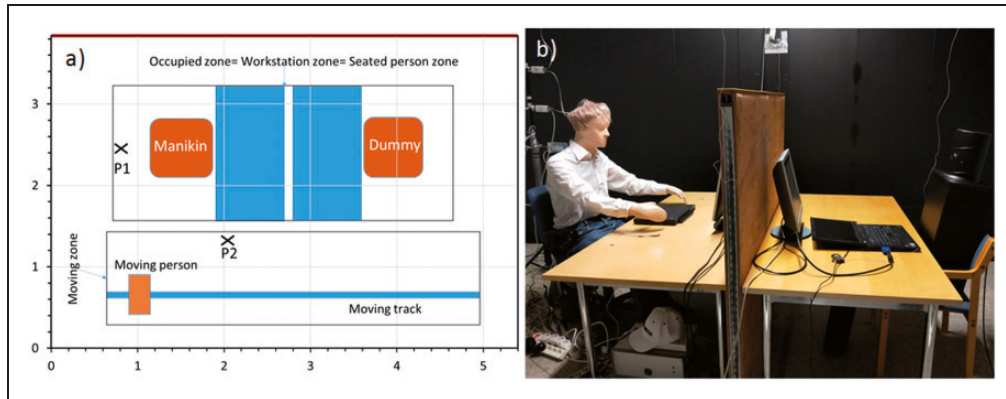


**Figure 4.** (a) The area of different zones in the chamber and (b) the seated dummy and manikin.  
Note: Please refer to the online version of the article to view the figures in colour.

**Table 2.** Heat gains per floor area, specific airflow rates and temperatures.

Case	Air flow rate (L/s·m <sup>2</sup> )	Supply air temperature (°C)	Total heat flux (W/m <sup>2</sup> )	Exhaust air reference temperature (°C)
1	3.7	17	40	26
2	5.6	17	60	26
3	7.3	17	80	26

between 3.7 and 7.3 L/s/m<sup>2</sup> according to heat gain. For internal heat gains, all electrical powers, e.g. lights, dummy, etc. were measured. The required heat gain balance was adjusted with the simulated window panel. The heating power of the window panel and the foil on the floor were adjusted to reach the set cooling load levels. In the case of 80 W/m<sup>2</sup>, the additional heat source of 0.4 × 0.4 × 0.4 m<sup>3</sup> was located on the floor below the table to model a computer, see Figure 2(a).

The parameters of the test cases are summarized in Table 2. The exhaust temperature was kept at 26°C as the reference temperature for all three heat gain levels.

In the tests, three moving speeds were used: 0.3 m/s, 0.6 m/s and 1.0 m/s. With 3 m length track, the speed of 1.0 m/s was the maximum that can be reached. However, the speed could be assumed to describe the normal walking speed in the office. The speeds of 0.3 m/s and 0.6 m/s were as reference speeds. So the simulated person took 20 s, 10 s and 6 s for one turn to move on the track. The simulated person moved by four cycle patterns: continuous moving and with 5 s, 10 s and 15 s interval breaks between each turn, as shown in Table 3. In this study, all together 81 cases were measured.

### Measurement instruments and measurement locations

In the test of moving person, different moving speeds and cycle patterns were measured to find how the

movement could disturb the air distribution. Two locations (P1 and P2) were measured with the air temperature and velocity, where P1 (length-coordinate 0.68 m, width-coordinate 2.4 m) was near the seated person zone and P2 (at length-coordinate 2.05 m, width-coordinate 1.44 m) was near the track (see Figure 2(a)).

Figure 2(b) shows the measured locations with steady-state conditions and the section A-A included the measurement locations of P2, P3 (corridor side) and P4 (simulated window side).

The characteristics of flow field were measured by seven hot-sphere anemometers at every measurement location. The anemometers were installed into a measuring mast at heights of 0.1 m, 0.6 m and 1.1 m according to recommendations given by the European Standard EN ISO 7726:1998.<sup>37</sup> Another four anemometers were measured at the height of 1.4 m, 1.7 m, 2.3 m and 2.9 m. Because of the limitation of measurement devices, two different sensors were used. Three lowest sensors were the Vivo Draught 20T31 anemometers with the sampling rate of 10 Hz. The four highest sensors were the wireless Sensoanemo 5100SF anemometers with the sampling rate of 0.5 Hz. The Sensoanemo and the Vivo Draught anemometers were calibrated before the measurement.

The Tinytag Plus-2-meters were attached to internal window and corridor side walls to measure near-wall temperature and relative humidity conditions.

**Table 3.** Moving speeds and interval brake times of the test cases.

Moving person state		Moving with stops in each turn (brake time)										
No moving	Continuous moving (Cont.)	1.0 m/s	0.6 m/s	0.3 m/s (5 s)	0.6 m/s (5 s)	1.0 m/s (5 s)	0.3 m/s (10 s)	0.6 m/s (10 s)	1.0 m/s (10 s)	0.3 m/s (15 s)	0.6 m/s (15 s)	1.0 m/s (15 s)
Steady state	0.3 m/s	0.6 m/s	1.0 m/s	0.3 m/s (5 s)	0.6 m/s (5 s)	1.0 m/s (5 s)	0.3 m/s (10 s)	0.6 m/s (10 s)	1.0 m/s (10 s)	0.3 m/s (15 s)	0.6 m/s (15 s)	1.0 m/s (15 s)

The uniformity of the surface temperature of the panel was measured with infrared camera and temperature sensors to verify that water circuit inside the panel is as designed. Indoor airflow pattern was visualized with marker smoke. This visualization was used to recognize air flow pattern. All the measurement devices used in the experiments are summarized in Table 4.

**Experimental procedure**

In the test, the room reached another quasi-steady state condition after the plate had moved for 10 min. All tests started under steady-state condition. In the measurements, the data acquired during 10 min period before starting the plate movement were averaged as the steady condition. The data collected during the 10 min dynamic tests were averaged as the simulated moving conditions, respectively. Thus, all the 10 min measurement periods were about 3.3 times longer than normally used, 3 min averaged measurements.<sup>39</sup>

**The thermal comfort indices and airflow characteristics**

In this study, the thermal conditions were analysed by using heat removal efficiency (HRE) and draught rate. HRE is an index used to evaluate the effectiveness of heat removal<sup>40</sup> and it was calculated by equation (1).

$$HRE = \frac{\bar{T}_{out} - \bar{T}_{in}}{T_{1.1} - \bar{T}_{in}} \tag{1}$$

where  $T_{1.1}$  (°C) is the mean air temperature at 1.1 m,  $\bar{T}_{out}$  (°C) is the exhaust temperature and  $\bar{T}_{in}$  is the mean supply air temperature. In this study, the height of 1.1 m was selected to describe the HRE. The 1.1 m is the height of the head level for a sitting person.<sup>36</sup> Also, this is the common height level for the room air sensor.

The walk of person increases the room air velocity as well as its fluctuation. The standard deviation (SD) of the velocity is defined by equation (2).

$$SD = \sqrt{\frac{\sum_{i=1}^N (u_i - \bar{u})^2}{N - 1}} \tag{2}$$

where  $\bar{u}$  is the mean air speed,  $u_i$  is the measured speed at the given time and  $N$  is the sample of the data set.

Draught is defined as an unwanted local cooling of the human body caused by the air movement, which is strongly related to local air speed. Standard EN ISO

**Table 4.** The measuring instruments.

Variable	Model	Accuracy
Air temperature and air velocity (at height of 0.1 m–1.1 m)	Dantec dynamics Vivo Draught 20T31	Air velocity (v): 0.05–1.0 m/s ±0.01 m/s ± 0.025; v <sub>meas</sub> temperature (t): 0–45°C ± 0.15°C; Sampling rate: 10 Hz
Air temperature and air velocity (at height of 1.4 m–2.9 m)	Sensor electronic SensoAnemo 5100SF	Air velocity (v): 0.05–5 m/s ± 0.02 m/s ± 0.015; v <sub>meas</sub> temperature (t): –10–50°C ± 0.2°C; Sampling rate 8 Hz
Airflow patterns	Tiny S and marker smoke	–
Surface temperature	ThermaCAM™ P60 infrared camera	±2°C or ±2%·T <sub>meas</sub> <sup>38</sup>
Pressure difference	Swema 3000	±0.3% of reading, lowest ± 0.3 Pa
Airflow rate	IRIS-200	±5%

7730:2005<sup>41</sup> defines the draught rate (DR) as given by equation (3).

$$DR = (34 - T_{a,l})(\bar{u}_{a,l} - 0.05)^{0.62}(0.37 \cdot \bar{u}_{a,l} \cdot Tu + 3.14) \quad (3)$$

where  $T_{a,l}$  is the local air temperature from 20°C to 26°C,  $\bar{u}_{a,l}$  is the local mean air speed from 0.05 m/s to 0.5 m/s, and  $Tu$  is the local turbulence intensity in per cent from 10% to 60%.

The turbulence intensity,  $Tu$ , is defined by equation (4).

$$Tu = \frac{u_{SD}}{\bar{u}} \times 100 \quad (4)$$

In this study, the airflow characteristics were analysed by equivalent frequency, turbulent kinetic energy, energy spectral distribution and fluctuation energy ratio.

The equivalent frequency ( $f_e$ ) is defined as a frequency of sinusoidal velocity fluctuations with the same ratio of the standard deviation of acceleration to the standard deviation of air velocity as in the random velocity fluctuations.<sup>42</sup> The equivalent frequency,  $f_e$ , is defined by equation (5).

$$f_e = \frac{1}{2\pi} \frac{SD_a}{SD} \quad (5)$$

where  $SD_a$  is the standard deviation of acceleration of velocity and  $SD$  is the standard deviation of the air velocity. The characteristics of the turbulent airflow can be described, e.g. by turbulence intensity, length scales, time scales and turbulent kinetic energy. The equivalent frequency was used together with turbulence intensity, mean velocity and air temperature to characterize sensation of draught.<sup>43</sup> The equivalent frequency is decreased with decreasing fluctuation of the force and is increased with decreasing fluctuation of air speed in the airflow. At this stage, the force that accelerates the

flow presumably decreases slightly with a lower thermal temperature. However, also the air velocity fluctuation may decrease slightly. The ratio of those parameters comes from the statistical airflow conditions, sampling rate and measured time-interval loads.

The turbulent kinetic energy,  $k_t$ ,<sup>44</sup> is approximated by equation (6).

$$k_t = \frac{1}{2} \overline{u'u'} \quad (6)$$

where  $u'$  is the fluctuation component of air speed when omnidirectional probe is used as a measurement.

The Fourier transform of airflow fluctuation represents a frequency distribution from the set of discrete values of a given variable over the time-interval by providing the sinusoidal components of original function with certain frequency. The Fourier transform,  $\hat{\phi}(\omega)$ , is expressed as equation (7).

$$\hat{\phi}(\omega) = \int_{-\infty}^{\infty} \phi(t)e^{-i\omega t} dt \quad (7)$$

where  $\phi$  is a set of measured air velocities in this study,  $\omega$  is angular frequency and  $t$  is time. The angular frequency is determined as  $\omega = 2\pi f$  and  $f = \frac{1}{T}$ , where  $f$  is the frequency.

The outcome of the Fourier transform is the complex-valued function  $\hat{\phi}(\omega)$ . The frequency distribution is then presented in a real number set by taking the absolute value  $|\hat{\phi}(\omega)|$  from the transformed function which shows the magnitude spectrum. Furthermore, the power spectrum is determined as  $|\hat{\phi}(\omega)|^2$ . The discrete Fourier transform,  $\hat{\phi}(f)_k$ , is defined by equation (8).

$$\hat{\phi}(f)_k = \sum_{j=1}^N \phi(t)_j e^{(-2\pi i(j-1)(k-1)/N)} \quad (8)$$

where  $j$  and  $k$  denotes the indexes and  $N$  is the sample of the discrete data set.

The power spectral density describes the distribution of power as a function of frequency that provides a normalized power spectrum. The power spectral density was calculated using the Fast Fourier Transform (FFT) method in Matlab software.<sup>45</sup> Consequently, the power spectral density,  $S(f)$ , is determined by equation (9).

$$S(f) = \frac{1}{N} |\hat{\mathcal{O}}(f)|^2 \quad (9)$$

where the divisor  $N$  normalize the result. The energy spectrum<sup>44</sup> is expressed as equation (10).

$$\int_0^{\infty} E(f) df = \overline{u'_i u'_i} \quad (10)$$

where  $u'_i$  is the fluctuation component of the air speed.

The equation shows the distribution density of velocity fluctuation in a range of frequencies, where  $E(f)$  is the spectral distribution function of  $\overline{u'_i u'_i}$ .

The fluctuation energy,  $F(E)$ , integral over the time is determined from a numerical integral as given by equation (11).

$$F(E) = \int_{t_1}^{t_2} u' u' dt \approx \sum_{i=1}^N (u' u')_i \Delta t_i \quad (11)$$

Furthermore, the fluctuation energy ratio,  $X(E)$ , for a certain time-series records is determined by equation (12).

$$X(E) = \frac{\sum_{i=1}^N (u' u')_i \Delta t_i}{\sum_{i=1}^N (uu)_i \Delta t_i} \quad (12)$$

that in turn shows the relative amount of fluctuation energy compared with kinetic energy including the mean airflow motions.

## Results

### Temperature

In the tests, three moving speeds 0.3 m/s, 0.6 m/s and 1.0 m/s were used for the simulated person. Also, the effect of intermittent movement of the simulated person with four different cycle patterns was tested. Figure 5 shows the temperature distribution in the section A-A (in the location of the measurement points P2, P3 and P4) and the adjacent zone of the manikin (in the point P1) under steady-state condition with the heat gain of 40 W/m<sup>2</sup> and 80 W/m<sup>2</sup>. At the steady state, the

more thermal load from heated window led to asymmetric load distribution. Then the upward buoyancy flow from the heated window pushed the air supplied from the diffuse ceiling to flow downward over the opposite wall. Thus, the air temperature near simulated window (P3) was higher than that at corridor side (P4) due to the effect of asymmetrical heat gains. With the heat gain of 40 W/m<sup>2</sup>, the air temperature was 0.7°C higher close to the window than that close to the corridor wall. With 80 W/m<sup>2</sup>, this air temperature difference was 1.0°C. This depicts the effect of asymmetric heat load distribution on the temperature profile where the location of the heat gain was the key factor.

The effect of the simulated moving person on the vertical air temperature is presented in Figure 5. In Figure 6, the average temperature distribution under the steady-state and dynamic conditions is shown with the constant moving speed of the simulated person (0.6 m/s). With a heat gain of 40 W/m<sup>2</sup>, the average air temperatures at P1 and P2 were rather similar in both steady-state and moving conditions (25.5°C). This means that the moving person has no significant effect on the vertical temperature gradient with the lower thermal load. However, with the heat gain of 80 W/m<sup>2</sup>, the moving person affected the room air temperature profile both in the occupied (P1) and near the simulated moving person (P2) zones. The mean air temperature at 1.1 m close to the workstation (P1) was 25.8°C under the dynamic condition, which was 0.2°C lower than with the steady-state condition. Nevertheless, the air temperature close to the track of the moving person (P2) was 0.2°C higher in the steady-state condition. In the case of no moving person, with asymmetric heat gain of 80 W/m<sup>2</sup>, there existed 1°C horizontal temperature difference. Due to the moving person, the horizontal temperature difference was reduced to 0.2°C. Thus, a moving person could reduce significantly the horizontal temperature difference.

The effect of the moving person on temperature profile was different with a heat gain of 40 W/m<sup>2</sup> and 80 W/m<sup>2</sup>. When the simulated person moves, the horizontal air mixing was enhanced between the occupied zone and moving zone. Therefore, the human movement would reduce the temperature at P1 but increased the temperature at P2. Due to a heat gain of 40 W/m<sup>2</sup>, there was less heat transfer between workstation and the side of the moving track than with a heat gain of 80 W/m<sup>2</sup>. Therefore, the human movement would reduce the temperature at P1 but would increase the temperature at P2. Under the dynamic condition, the vertical air temperature difference between 0.1 m and 0.6 m was 0.4°C at P1, and was 0.1°C at P2. This indicates that the moving person disturbed the thermal stratification near the moving person at P2.

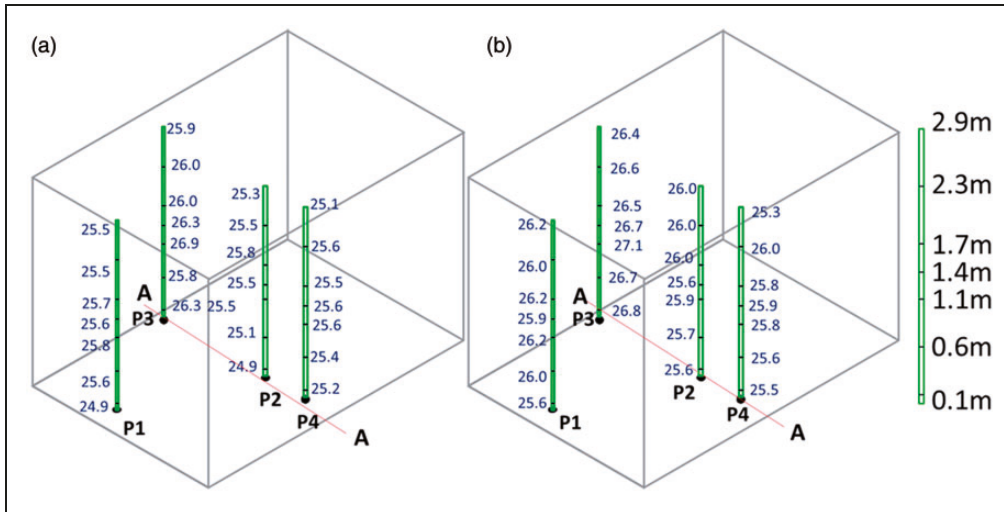


**Figure 5.** The air temperature distribution at the section A-A (points P2, P4 and P3) and near the manikin (point P1) under the steady state condition with the heat gain of (a) 40 W/m<sup>2</sup> and (b) 80 W/m<sup>2</sup>.

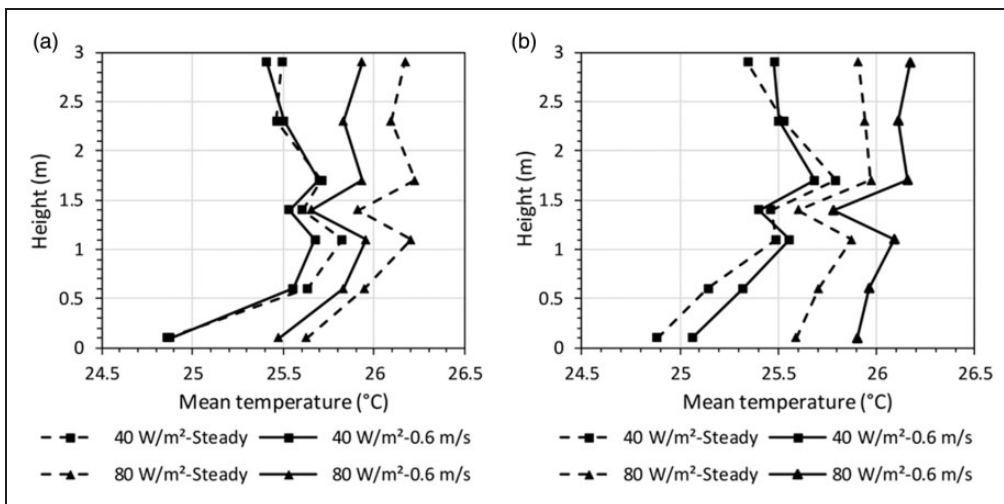


**Figure 6.** Mean air temperature with heat gains of 40 W/m<sup>2</sup> and 80 W/m<sup>2</sup> under steady-state conditions with a constant moving speed of 0.6 m/s (a) at point P1 (near manikin) and (b) at point P2 (near track).

The effect of the moving speed and moving cycle patterns on the vertical temperature gradient was studied. In Figure 7, the air temperature was increased at a distance from the ankle (0.1 m) up to the head height (1.1 m) of a seated person. Figure 7(a) shows that there was not much difference in air temperature profile caused by the various moving speeds. The lower moving speed had led to a slightly higher temperature at 0.6 m and 1.1 m. Figure 7(b) shows the moving frequency also had no significant effect on the air temperature profile. In the continuous moving case (0.6 m/s), the mean air temperature was 0.3°C lower than moving with intervals at heights of 0.6 m and 1.0 m. The air temperature at occupied zone was just slightly higher with a longer

stop interval (15 s) than with a shorter stop interval (5 s). Hence, different stop intervals did not have significant difference on the temperature profile. Also, there existed a clear difference only in the continuous moving case. In cases with breaks, there was no clear difference in vertical temperature gradient. This means only the continuous moving person has an effect on the vertical temperature gradient close to the workstation. In Figure 8, the induced airflow behind the simulated moving person is illustrated. When the simulated person moved, the significant effect on air movement was noted. These airflow patterns would affect the micro-environment close to the work station. By the effect of the induced air movement, the vertical

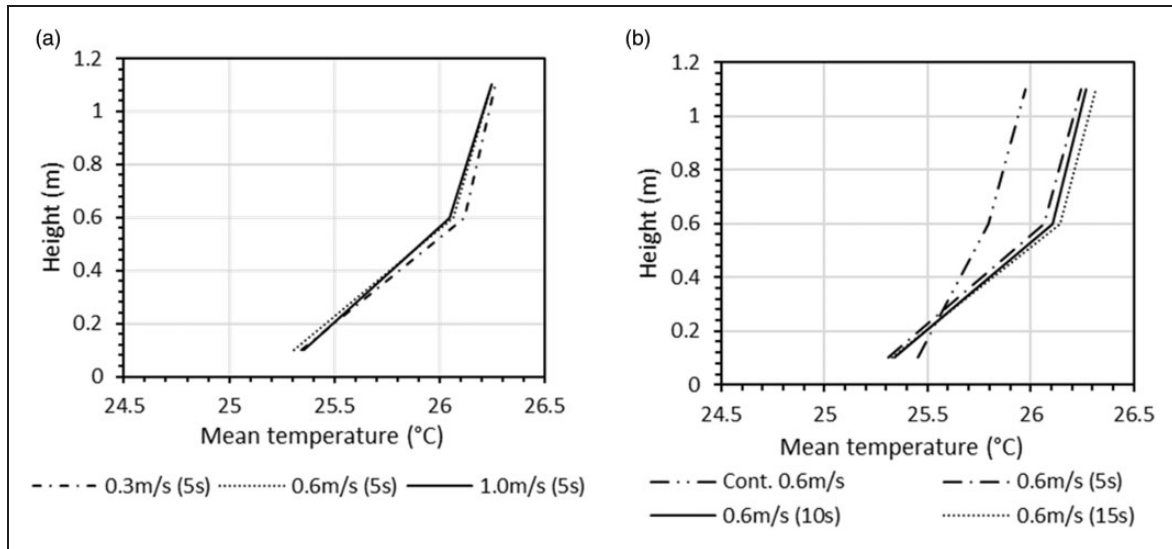


**Figure 7.** The mean air temperature profiles with  $80 \text{ W/m}^2$  between 0.1 m to 1.1 m at the point of P1 (near manikin) with (a) different moving speeds and (b) different stop intervals with moving speed of 0.6 m/s.

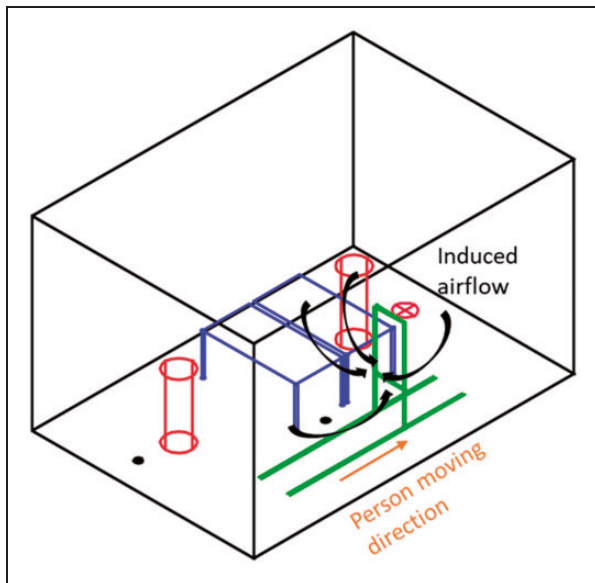


**Figure 8.** The air distribution affected by the induced air movement of a moving person.  
 Note: Please refer to the online version of the article to view the figures in colour.

temperature gradient that was normally created in the steady-state condition was effectively reduced.

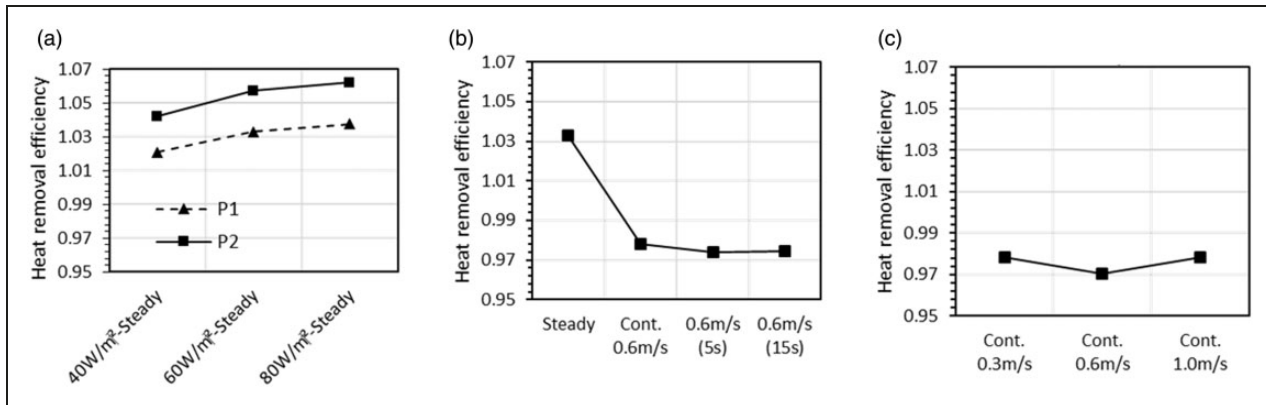
**Heat removal efficiency**

Figure 9 shows the HRE by using equation (1), when the exhaust temperature was constant. Figure 9(a) shows the average HRE under the steady-state condition with three different heat gain levels. The HRE was

greater close to the track (P2) than close to the manikin (P1) (Figure 8(a)), as the mean temperature at P1 was higher than P2. Compared with the steady-state condition under  $40 \text{ W/m}^2$ , HRE was reduced by 6% in the continuous moving (0.6 m/s) case (Figure 9(b)). The varied intervals of the simulated moving person did not have any influence on the HRE. Also, the moving speed did not have an effect on the HRE (Figure 9(c)). Because the moving person would cause a change in the air distribution and further the air temperature at 1.1 m level with constant exhaust temperature, the HRE was changed according to equation (1). Two factors were shown to reduce the HRE: the heat gain level and the moving person. However, the moving speed and stop interval did not have much effect on HRE. In all moving cases, HRE was at level of 0.97.

**Velocity profile**

According to European design criteria of CR1752,<sup>46</sup> for the indoor environment, the indoor climate categories A, B and C allow local air velocities of 0.15 m/s, 0.18 m/s and 0.21 m/s, respectively. Figure 10 shows mean air velocities with heat gains of  $40 \text{ W/m}^2$  to  $80 \text{ W/m}^2$  at 1.1 m. The minimum realistic absolute expanded uncertainty at the 95% confidence for the mean air velocity was  $dU = \pm(0.025 + 0.025 U)$ .<sup>47</sup> This means that the typical mean air velocity levels are correspondingly, e.g.  $0.1 \pm 0.028 \text{ m/s}$  and  $\pm 28\%$  and  $0.2 \pm 0.03 \text{ m/s}$  and  $\pm 15\%$ , respectively. Consequently, the relative uncertainty would be increased towards a lower air velocity level and would dominate the uncertainty of functions on air-flow characteristics.



**Figure 9.** Heat removal efficiency with respect to the (a) heat gain from  $40 W/m^2$  to  $80 W/m^2$  under the steady-state condition at P1 (near manikin) and P2 (near track), (b) different stop intervals with a heat gain of  $40 W/m^2$  at P1 (near manikin) and (c) different moving speeds with a heat gain of  $40 W/m^2$  at P1 (near manikin).

Due to the person's movement, the mean air velocity was  $0.040 \pm 0.026 m/s$  at P1 with a heat gain of  $40 W/m^2$  and it was increased by 57% to  $0.063 \pm 0.027 m/s$  with a heat gain of  $80 W/m^2$ . In general, the mean air velocities were low in the seated person zone. However, the corresponding value was  $0.23 m/s$  with a heat gain of  $40 W/m^2$  and was increased by 15% to  $0.27 m/s$  with a heat gain of  $80 W/m^2$  near the moving track (P2). Compared to the seated person zone, the moving person increased the air velocity close to the moving simulated person more than 75%. This indicates the effect of the moving person on the air distribution in the room space. Due to the diffuse ceiling ventilation, the mean air velocity at the occupied zone can fulfil the Category A when the person moves about in the office. This indicates that with uniform air distribution by the diffuse ceiling ventilation, acceptable air velocity at occupied zone is possible under dynamic moving person condition.

The average air velocity was  $0.05 \pm 0.026 m/s$  and  $0.07 \pm 0.027 m/s$  with the continuous moving speeds of  $0.3 m/s$  and  $1.0 m/s$  with a heat gain of  $40 W/m^2$ . Therefore, the average air velocity was increased when the moving speeds of the simulated person were increased. Furthermore, the mean air velocity with the continuous moving simulated person was much higher than with interval breaks between each turn.

In all cases, the effect of moving person was small on the mean air velocity close to the workstation. Thus, the moving speed and stop intervals did not have an effect on the air velocity. The strength of the heat gain had some effect on the average air velocity. However, all cases fulfilled the demand of Category A.

### Air velocity fluctuation

The air velocity fluctuation (SD) is presented in Figure 10. Figure 11(a) shows the increase of air

velocity fluctuation with different cooling load levels. In the seated person zone (P1), the standard deviations of the instantaneous air speed were  $0.05 m/s$  and  $0.06 m/s$  with heat gains of  $40 W/m^2$  and  $80 W/m^2$ , respectively. Thus, the standard deviation was increased by 24% with heat gains of  $40 W/m^2$  to  $80 W/m^2$ . The corresponding standard deviations were  $0.16 m/s$  ( $40 W/m^2$ ) and  $0.20 m/s$  ( $80 W/m^2$ ) close to the track at P2. As could be expected, this means that the moving person has more significant influence on the air velocity fluctuation near the moving track than the workstation. Also, the heat gain level had caused an increase in the standard deviation of air velocity close to the workstation.

Figure 11(b) shows the continuous moving of the simulated person, which made the air flow most turbulent. The SD was reduced slightly when longer speed-breaks existed. The fluctuation was higher with the continuous moving than with stop intervals cases. The average SD almost increases linearly with the increasing moving speed (Figure 11(c)).

### Equivalent frequency

Table 5 shows the equivalent frequency defined by equation (5) with different measured cases near the work station at P1. The equivalent frequency did not change much when the heat gain varied from  $40 W/m^2$  to  $80 W/m^2$  at workstation area. Also, the lower moving speed ( $0.3 m/s$ ) of a moving person with a heat gain of  $80 W/m^2$  did not cause much difference on equivalent frequency. However, when the moving speed was increased to  $1.0 m/s$ , the equivalent frequency was increased by 32% (from  $0.43 Hz$  to  $0.64 Hz$ ). The relative effect was at the same level than in mean velocity. The moving pattern with a speed-break also caused an increase in the equivalent frequency by 40% (from

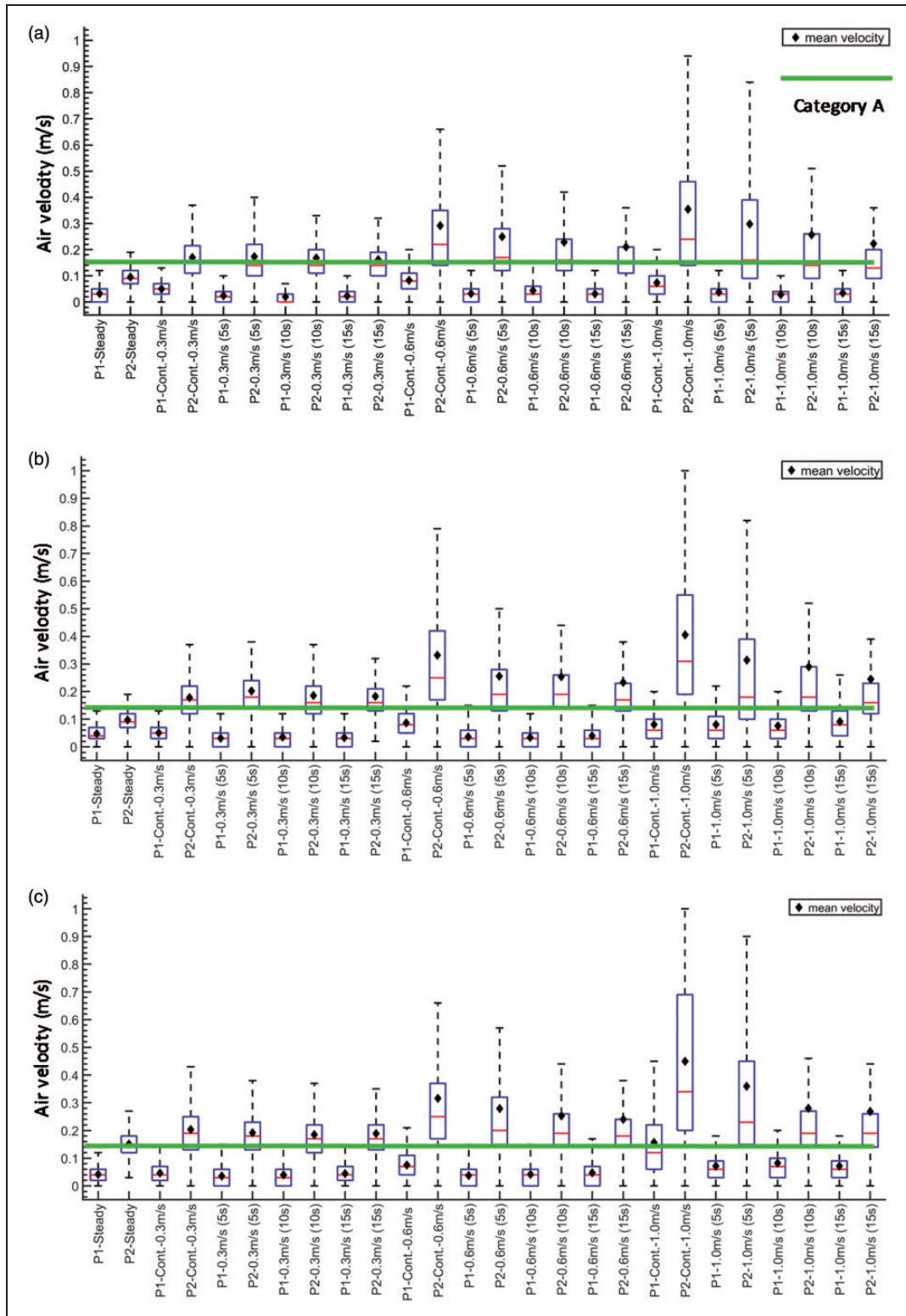


**Figure 10.** Air velocities at a height of 1.1 m at P1 (near manikin) and P2 (near track) with a heat gain of (a)  $40 \text{ W/m}^2$ , (b)  $60 \text{ W/m}^2$  and (c)  $80 \text{ W/m}^2$ . The box indicates the 25th percentile, median and 75th percentile of spatial mean air velocities. The whiskers denote a range of mean air velocities excluding the outliers. The x-axis denotes 26 different measuring cases.

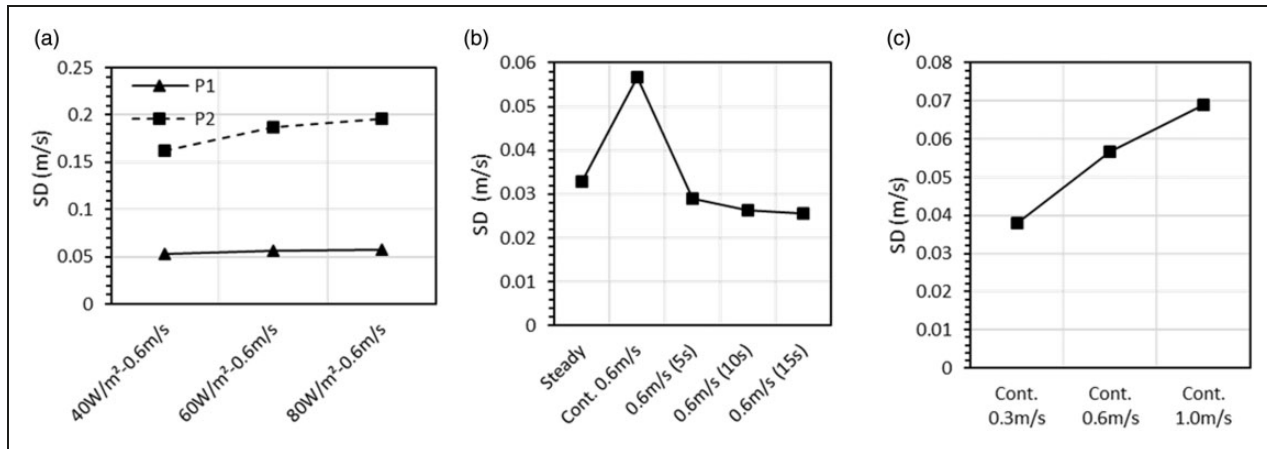


**Figure 11.** Standard deviation of air velocity with (a) heat gains of 40 W/m<sup>2</sup> to 80 W/m<sup>2</sup> at P1 and P2 with constant moving of a person at a moving speed of 0.6 m/s, (b) different moving frequencies at P1 with a heat gain of 60 W/m<sup>2</sup> and (c) different moving speeds with a heat gain of 60 W/m<sup>2</sup> at P1.

**Table 5.** The equivalent frequency with different cases at P1.

	Equivalent frequency at different measured cases		
Moving pattern	Steady at 80 W/m <sup>2</sup> 0.43	Cont. 1.0 m/s at 80 W/m <sup>2</sup> 0.64	1.0 m/s (15 s) at 80 W/m <sup>2</sup> 0.72
Moving speed	Cont. 0.3 m/s at 80 W/m <sup>2</sup> 0.43	Cont. 0.6 m/s at 80 W/m <sup>2</sup> 0.53	Cont. 1.0 m/s at 80 W/m <sup>2</sup> 0.64
Cooling load	Steady state at 40 W/m <sup>2</sup> 0.42		Steady state at 80 W/m <sup>2</sup> 0.43

0.43 Hz to 0.72 Hz). The relative effect was smaller in comparison to the mean velocity (70%). The equivalent frequency near the moving area (0.78 Hz) was higher than at occupied zone (0.64 Hz). Therefore, as would be expected, the air flow pattern was more stable at the occupied zone. As a conclusion, the continuous moving speed of a moving person and moving with stop intervals would increase the equivalent frequency. However, the cooling load did not have any influence.

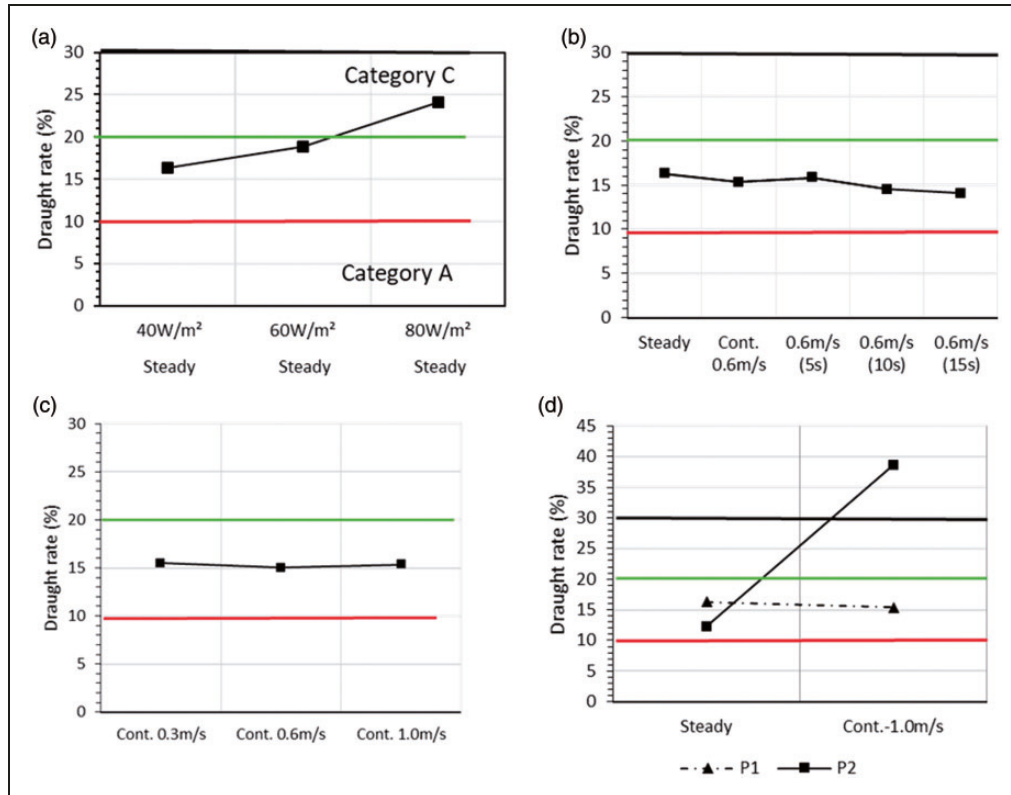
### Draught rate

Figure 11 shows the maximum draught rate at 1.1 m at locations P1 and P2. The average draught rate at the seated person zone was 16.3% and 24.0% with cooling loads of 40 W/m<sup>2</sup> and 80 W/m<sup>2</sup> under the steady-state condition (Figure 12(a)). The uncertainty of draught rate at P1 was 4–5%.<sup>47</sup> Therefore, the thermal environment was classified as categories B and C according to the EN ISO 7730:2005.<sup>40</sup> The draught rate at P1 was increased by 32% when the heat gain was increased from 40 W/m<sup>2</sup> to 80 W/m<sup>2</sup>. The air velocity was increased as a function of the heat gain. This indicates that the heat gain has a direct effect on the draught rate

and with a heat gain of 80 W/m<sup>2</sup>, only category B was fulfilled.

Figure 12(b) shows that the draught rate at P1 was slightly lower with the moving person than in the steady-state condition. The air velocity at P1 was very low (below 0.15 m/s) in all moving cases. The reason for the draught rate reduction is that the mean air temperature was lower at P1 with the moving person. This indicates that in certain conditions the diffuse ceiling ventilation could reduce the local thermal comfort with a moving person in the workstation area.

However, the moving of the person with different time intervals did not have much effect on the draught rate compared with continuous moving. Also, the average draught rate did not change much when the moving speed was increased from 0.3 m/s to 1.0 m/s with a heat gain of 40 W/m<sup>2</sup> (Figure 12(c)). Figure 11(d) shows that the trend of the average draught rate at P2, which was increased as a function of the moving speed. This indicates that the moving person has a significant influence on the draught rate near the moving track, but only a minor influence at the occupied zone when the diffuse ceiling ventilation was used.



**Figure 12.** Draught rate at 1.1 m with (a) heat gains of 40 W/m<sup>2</sup> to 80 W/m<sup>2</sup> under the steady-state condition, (b) different moving frequencies with a heat gain of 40 W/m<sup>2</sup> at P1 (near manikin), (c) different moving speeds with a heat gain of 40 W/m<sup>2</sup> at P1 (near manikin) and (d) at different measured locations with a heat gain of 40 W/m<sup>2</sup> under steady-state and constant moving condition close to manikin (P1) and track (P2).

Note: Please refer to the online version of the article to view the figures in colour.

### Power spectral density

Figures 13 and 14 show the fluctuation energy defined by equation (9) at heights 1.1 m and 0.1 m, respectively. Table 6 shows the average fluctuation energy in different cases near the work station at P1. The Fourier transform produces a spectrum up to 10 Hz, because the spectrum is symmetric about a half of a sampling frequency.<sup>48</sup> Hence, Figure 12 shows the fluctuation energy as a function of frequency up to 5 Hz, i.e. half of a sampling rate due to the Nyquist frequency.<sup>49</sup>

Figure 13 shows that the frequency distribution follows reasonably well the Kolmogorov law. The dashed line describes the  $-5/3$  law<sup>46</sup> for the cascading process in turbulence at the height of 1.1 m. Most of the turbulent energy was concentrated at low frequencies. Figure 13(a) shows average power spectral density was  $1.8 \times 10^{-3} \pm 7.8 \times 10^{-2} \text{ m}^2/\text{s}^2$  in the occupied zone (P1) at the height of 1.1 m with the case of 40 W/m<sup>2</sup> in the steady-state condition. The corresponding average power spectral density was  $2.9 \times 10^{-3} \pm 1.4 \times 10^{-1} \text{ m}^2/\text{s}^2$  at 80 W/m<sup>2</sup>. Consequently, the average fluctuation energy increased by 46% when the heat gain changed from 40 W/m<sup>2</sup> to 80 W/m<sup>2</sup>. The relative effect

of increased heat gain was therefore greater than the standard deviation of 24%. Figure 13(b) shows that the power spectral density with the continuous moving person was the largest. Compared to the steady-state condition, the mean value was increased by 93% (both fluctuation energy and standard deviation) up to  $4.2 \times 10^{-2} \pm 1.9 \text{ m}^2/\text{s}^2$  with the continuous moving person (0.6 m/s). Figure 13(c) shows the average power spectral density at the occupied zone (P1) with the different continuous moving speed in the case of 80 W/m<sup>2</sup>. The average energy was  $3.6 \times 10^{-3} \pm 1.6 \times 10^{-1} \text{ m}^2/\text{s}^2$  with the moving speed of 0.3 m/s, and was increased by 91% with the moving speed of 1.0 m/s. Figure 13(d) shows that the fluctuation energy near the moving track (P2) was much higher, as would be expected, than at the seated person zone (P1). The average value was  $3.4 \times 10^{-2} \pm 1.8 \text{ m}^2/\text{s}^2$  at P2, while the corresponding value was  $4.1 \times 10^{-3} \pm 1.3 \times 10^{-1} \text{ m}^2/\text{s}^2$  at P1 with 80 W/m<sup>2</sup>. Therefore, there was a significant difference of the airflow characteristic between the seated person zone and moving zone. As a conclusion, the power spectral density was increased significantly when the moving speed was increased. In cases of stop intervals, the power

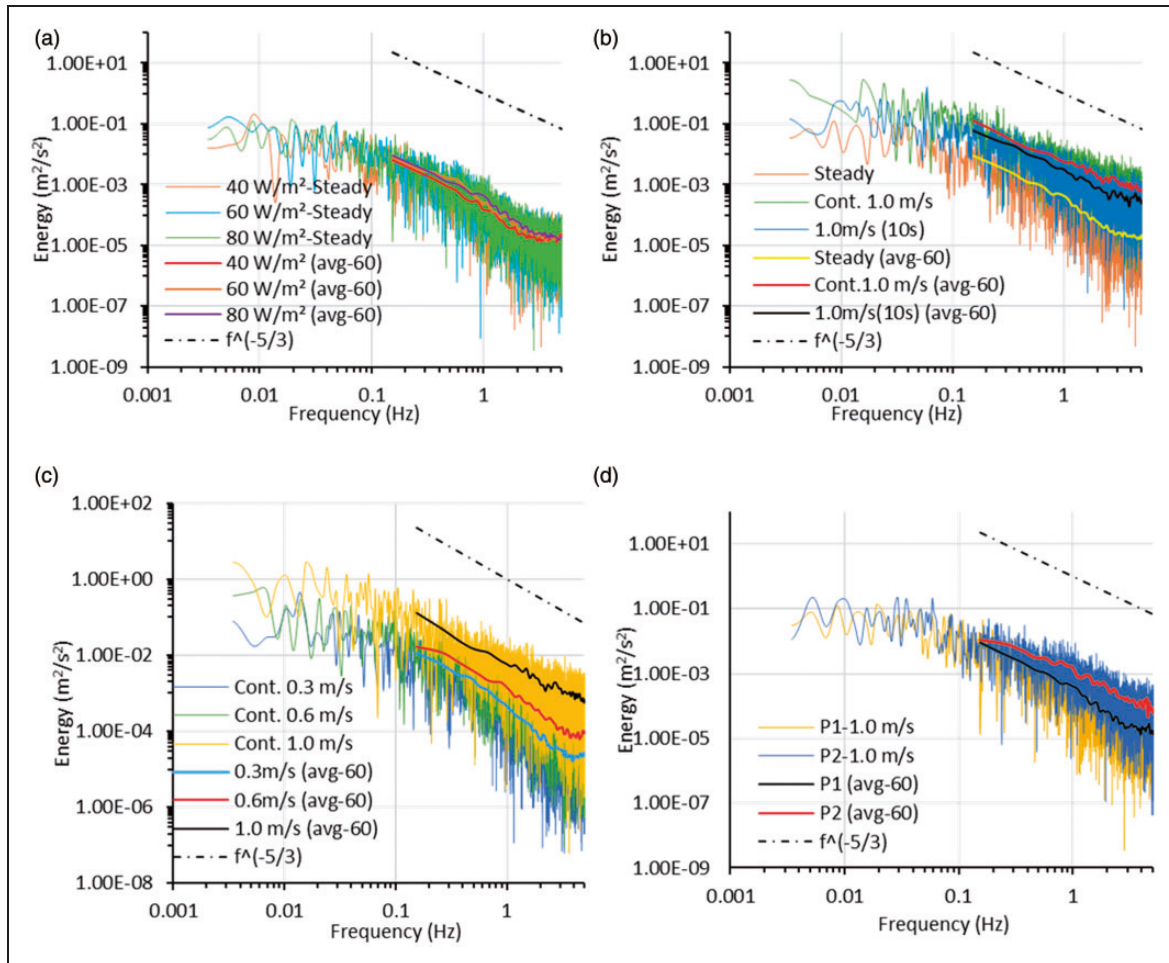


**Figure 13.** The fluctuation energy at a height of 1.1 m, log-log scales: (a) a heat gain from  $40 \text{ W/m}^2$  to  $80 \text{ W/m}^2$  in the steady-state condition, (b) different moving frequencies with a heat gain of  $80 \text{ W/m}^2$ , (c) different moving speeds with a heat gain of  $80 \text{ W/m}^2$  and (d) at different measured points with a heat gain of  $80 \text{ W/m}^2$  and a moving speed of  $1.0 \text{ m/s}$  (15 s). (avg-60) means the average value of the numerical field being evaluated within the time range analysed. Note: Please refer to the online version of the article to view the figures in colour.

spectral density was slightly lower than with continuous moving case.

The average power spectral density at the height of  $0.1 \text{ m}$  had the same trend than at  $1.1 \text{ m}$  (Figure 14). The average fluctuation energy was increased by 34% with the increasing heat gain. However, the moving frequency has less influence on the power spectral at a height of  $0.1 \text{ m}$  than at a height of  $1.1 \text{ m}$ . Also, the energy distribution varied almost according to  $k^{-1}$  at a height of  $0.1 \text{ m}$ . This indicated strong interaction between thermal plume and air movement caused by person walking.

### Turbulent kinetic energy

Figure 15 shows the average turbulent kinetic energy ( $k_t$ ) by using the equation (6) where the turbulent energy was increased with a higher thermal load

level, higher moving frequency and higher moving speed. The turbulent kinetic energy was on average  $1.1 \times 10^{-3} \text{ m}^2/\text{s}^2$  in the case of a heat gain of  $40 \text{ W/m}^2$  at a height of  $1.1 \text{ m}$  (Figure 15(a)). The turbulent kinetic energy was on average 35% higher with a heat gain of  $80 \text{ W/m}^2$  than with  $40 \text{ W/m}^2$ . This indicates an increase of turbulent kinetic energy when the thermal load was increased.

The average turbulent kinetic energy was  $1.8 \times 10^{-3} \text{ m}^2/\text{s}^2$  in the steady-state condition (Figure 15(b)) at  $1.1 \text{ m}$ . The corresponding energy was increased by 93% with the continuous moving person. However, the turbulent kinetic energy was reduced by 60% to  $1.0 \times 10^{-2} \text{ m}^2/\text{s}^2$  with a moving interval of 10 s. At a height of  $0.1 \text{ m}$ , the average turbulent kinetic energy was highest with the continuous moving condition. Figure 15(c) shows the average turbulent kinetic

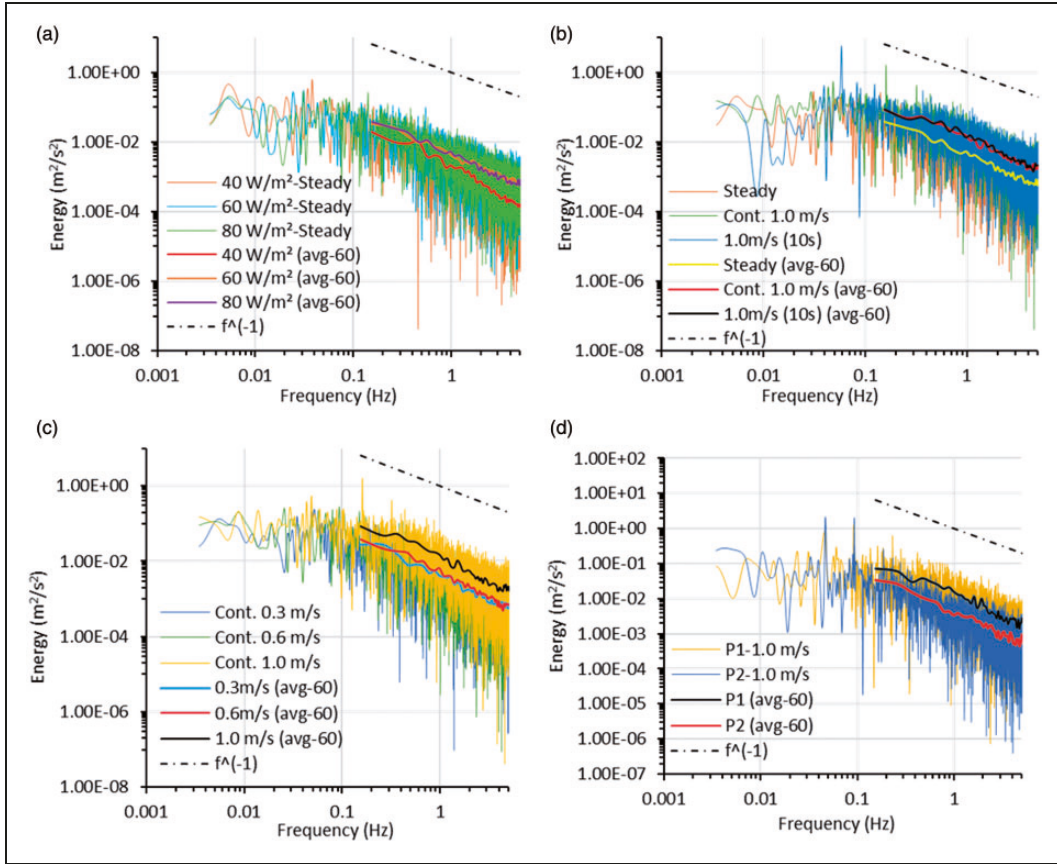


**Figure 14.** The fluctuation energy at a height of 0.1 m, log-log scales: (a) a heat gain of 40 W/m<sup>2</sup> to 80 W/m<sup>2</sup> in the steady-state condition, (b) different moving frequencies with a heat gain of 80 W/m<sup>2</sup>, (c) different moving speeds with a heat gain of 80 W/m<sup>2</sup> and (d) at different measured locations with a heat gain of 80 W/m<sup>2</sup>–1.0 m/s (15 s). (avg-60) means the average value of the numerical field being evaluated within the time range analysed. Note: Please refer to the online version of the article to view the figures in colour.

**Table 6.** The average power spectral density with different test cases at P1.

	1.1 m (head level)			0.1 m (ankle level)		
	40 W/m <sup>2</sup>	60 W/m <sup>2</sup>	80 W/m <sup>2</sup>	40 W/m <sup>2</sup>	60 W/m <sup>2</sup>	80 W/m <sup>2</sup>
	Steady state					
Heat gain						
Power spectral density (m <sup>2</sup> /s <sup>2</sup> )	1.79E-03	3.33E-03	2.94E-03	3.41E-03	4.89E-03	5.14E-03
SD of power spectral density (m <sup>2</sup> /s <sup>2</sup> )	7.83E-02	1.71E-01	1.35E-01	1.96E-02	1.50E-02	1.64E-02
Moving pattern	Steady state	Cont. 1.0 m/s	1.0m/s (10s)	Steady state	Cont. 1.0 m/s	1.0m/s (10 s)
Power spectral density (m <sup>2</sup> /s <sup>2</sup> )	2.92E-03	4.16E-02	1.37E-02	2.92E-03	4.16E-02	1.37E-02
SD of power spectral density (m <sup>2</sup> /s <sup>2</sup> )	1.34E-01	1.87E+0	5.22E-01	1.34E-01	1.87E+0	5.22E-01
Moving speed	Cont. 0.3 m/s	Cont. 0.6 m/s	Cont. 1.0 m/s	Cont. 0.3 m/s	Cont. 0.6 m/s	Cont. 1.0 m/s
Power spectral density (m <sup>2</sup> /s <sup>2</sup> )	3.63E-03	8.91E-03	4.20E-02	4.76E-03	6.01E-03	1.34E-02
SD of power spectral density (m <sup>2</sup> /s <sup>2</sup> )	1.62E-01	4.34E-01	1.87E+0	1.43E-02	1.91E-02	4.69E-02

SD: standard deviation.

energies close to the manikin (P1) were  $2.2 \times 10^{-3} \text{ m}^2/\text{s}^2$  and  $2.6 \times 10^{-2} \text{ m}^2/\text{s}^2$  with a moving speed of 0.3 m/s and 1.0 m/s at a height of 1.1 m. The relative difference was 91% at a height of 1.1 m. Similarly, the

difference was 67% at 0.1 m height, which indicates that the moving speed has a significant effect on the turbulent kinetic energy. The turbulent kinetic energy near the moving track was 48% higher than

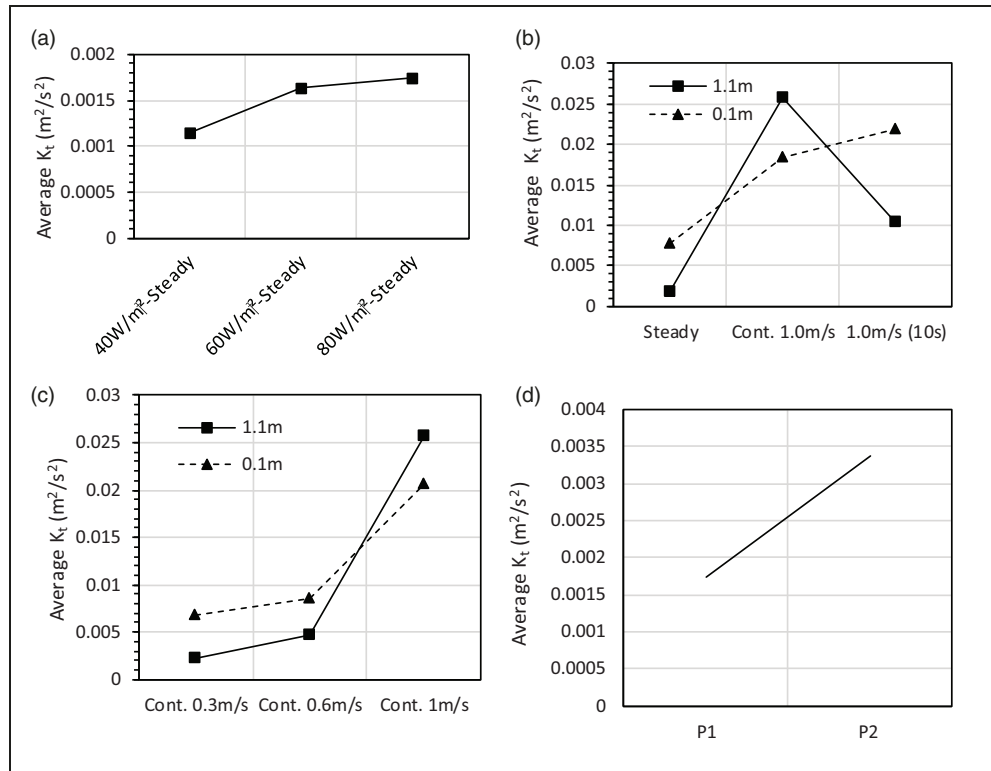


**Figure 15.** The average turbulent kinetic energy: (a) a heat gain of  $40 \text{ W/m}^2$  to  $80 \text{ W/m}^2$  at the steady-state condition at P1 (close to the manikin) at a height of 1.1 m, (b) different moving frequencies with a heat gain of  $80 \text{ W/m}^2$  at P1 (close to the manikin) at heights of 0.1 m and 1.1 m, (c) different moving speeds with a heat gain of  $80 \text{ W/m}^2$  at P1 (close to the manikin) at a height of 0.1 m and 1.1 m and (d) different measurement locations with a heat gain of  $80 \text{ W/m}^2$  in the case of  $1.0 \text{ m/s}$  (15 s) at a height of 1.1 m.

that at the seated person zone. Hence, as expected, the airflow was more turbulent near the moving person (Figure 15(d)). As a conclusion, the moving person has a higher effect on the turbulent kinetic energy than the increasing heat gain. With a continuous moving speed of  $1.0 \text{ m/s}$ , the turbulent kinetic energy was at the highest. The stop intervals would reduce the values but still the values were higher than the steady state.

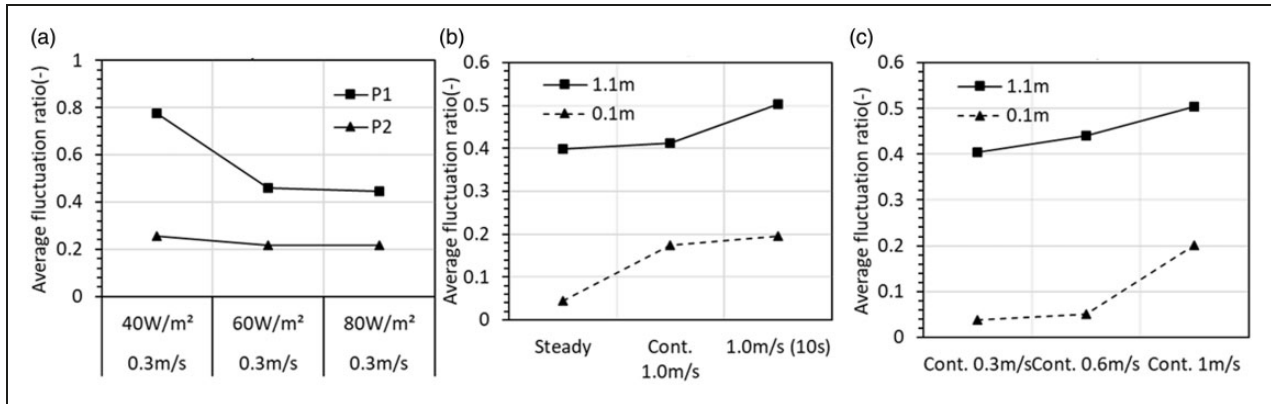
### Fluctuation energy ratio

Figure 16 shows the fluctuation energy ratio by using equation (12). In the case of a heat gain of  $40 \text{ W/m}^2$ , the fluctuation energy ratio was 0.78 at a height of 1.1 m close to the seated person zone (P1) (Figure 16(a)). This indicates that the amount of airflow fluctuation energy was approximately 78% of the airflow motions. Furthermore, the corresponding fluctuation energy ratio was 77% smaller with a heat gain of  $80 \text{ W/m}^2$  than with a heat gain of  $40 \text{ W/m}^2$ . This implies that the fluctuation energy was reduced as a function of the heat gain level.

However, the fluctuation energy ratio was much smaller at P2 (close to the track) than close to manikin (P1). This indicates that the moving person created more energy fluctuation at the seated person zone than near the moving track. Compared with the steady-state condition, the fluctuation energy ratio was 26% higher with the moving speed of  $1.0 \text{ m/s}$  (10 s) at the seated person zone at a height 1.1 m (Figure 16(b)). This means the moving person with the speed-break would create more energy fluctuation. The fluctuation energy ratio is much smaller at a height of 0.1 m, which indicates that less energy fluctuation was achieved at the ankle level. Figure 16(c) shows that the fluctuation energy ratio was highest with the moving speed of  $1.0 \text{ m/s}$  at both heights of 0.1 m and 1.1 m.

### Discussion

The main purpose of this study was to obtain an insight of the influence of human moving on air distribution and local thermal comfort with a diffuse ceiling ventilation system. The geometry of the simulated person



**Figure 16.** The fluctuation energy ratio: (a) heat gain from 40 W/m<sup>2</sup> to 80 W/m<sup>2</sup> with continuous moving speed at 0.3 m/s at the height of 1.1 m, (b) different moving frequency with 80 W/m<sup>2</sup> at P1 (close to the manikin) at the height of 0.1 m and 1.1 m and (c) different moving speeds with 80 W/m<sup>2</sup> at P1 (close to the manikin) at the height of 0.1 m and 1.1 m.

was selected according to Nordtest.<sup>35</sup> The person was simulated as a plate (1.6 m × 0.5 m × 0.03 m). The used plate in the experiment was different than the shape of a real human body, which would affect the airflow characteristic in the ventilated room. The previous studies has already demonstrated that the moving arms and legs of a real person could have an effect on air distribution close to workstation compared with the simulated person used.<sup>19,50</sup> The real human movement may create more a complicated induced airflow behind the moving body. Also in this study, the moving plate was not heated. However, the heat load of the real person would create a buoyancy flow (driven by convection heat flux) around the body that has also an effect on the air distribution. Nevertheless, the heat gain of the person (about 50 W is convection) is not so significant as compared with the other heat gains e.g. solar and equipment (1445 W).

The maximum moving speed of a simulated person was 1.0 m/s in this study because of geometry limitation of the test chamber. The higher moving speed would increase the mixing effect from both vertical and horizontal directions. In the office with diffuse ceiling ventilation, the horizontal temperature gradient is typically higher than 2°C.<sup>9</sup> Thus, the temperature gradient could be expected to be smaller in the higher moving speed condition.

The effect of a moving person on the different air distribution methods is different. Compared with stratum ventilation and displacement ventilation, the influence with mixing ventilation is the smallest. The influence with stratum ventilation is smaller than that with displacement ventilation.<sup>27</sup> With airflow from the diffuse ceiling ventilation, the effect of a moving person on indoor airflow characteristic depends on the space dimensions. The indoor environment near the moving track is much more influenced by moving person than close to the workstation.

For draught sensation, the previous experiments had shown that individuals are more sensitive to the draught risk with the equivalent frequency between 0.2 and 0.6 Hz than the other frequency levels.<sup>41,42</sup> In this study, the equivalent frequency was mostly between 0.4 and 0.6 Hz at occupied zone. However, the mean air velocity was below 0.1 m/s. Thus, the draught rate still stayed at low level.

With displacement ventilation, the spectral distribution of the turbulent energy depends on the examined location, e.g. the distance from the outlet and the height above the floor.<sup>51</sup> In the case of the laminar flow in a clean room, the energy distribution is low, but it stays similar in a wide range of frequency.<sup>43</sup> As for the stratum ventilation, the spectral distribution of the velocity fluctuation depends on the horizontal distance from the supply terminal and height above the floor.<sup>52</sup> For locations close to supply terminals, the turbulence structure is influenced by the characteristic length scale of the supply diffusers. With the airflow development, the turbulence structure shifts to the similar power spectrum as that of a fully developed turbulent flow. The turbulence at head level is not yet fully developed under stratum ventilation.

In this study with a moving person under diffuse ceiling ventilation, the frequency distribution follows reasonably the  $k^{-5/3}$  law at 1.1 m and  $k^{-1}$  at 0.1 m. This is in good agreement with the experimental with the mixed ventilation.<sup>43</sup> Therefore, the turbulence energy spectrum is similar to those in a fully developed turbulent flow.

The results are not universal for all ventilation systems, the heat gain level and room layout. With the DCV, the cooling load level, dimension of the room and other disturbances, e.g. the moving person are the key factor that could affect the air movement and

the local thermal comfort. This means that the results are valid only with the given experimental set-up. Thus, the effect of a moving person is probably different with other types of air distribution system.

The most suitable application of the DCV is offices. Diffuse ceiling ventilation was able to maintain a suitable thermal comfort in the indoor environment with a moving person, especially with high thermal loads. With a heat gain of 80 W/m<sup>2</sup> when the supply air flow rate of DCV was 7.3 L/s/m<sup>2</sup>, the moving person did not increase significantly the draught risk close to the workstation.

For the future research, various moving speeds, interval time and indoor activities need to be investigated with advanced air distribution and cooling systems. The novel micro-environment system where part of the cooling is provided by radiation should be further analysed with the moving person.

## Conclusion

The effect of the human movement on the performance evaluation of diffuse ceiling ventilation was studied by means of an experiment, using a simulated moving person designed to go back and forth on a straight track using a trolley. The trolley was controlled with different moving speeds and stop time intervals during each turn. The conclusion based on the results is indicated as follows:

- The human movement had some effect on the vertical temperature gradient between the floor level and 0.6 m height. The temperature gradient was 0.4°C at occupied zone from 0.1 m to 0.6 m, but nearly no difference in the temperature gradient at the moving zone. The moving frequency had significant effect on the air temperature profile.
- As for the local thermal comfort, the draught rate was constant with a person moving at occupied zone. Results show that the diffuse ceiling ventilation was not very sensitive to turbulence even when an occupant moves in the office. The moving person would create a different airflow characteristic close to work stations and the moving person zone with the diffuse ceiling ventilation. In all cases, the mean velocity and draught rate were within the acceptable range at occupied zone with different moving speeds and moving patterns.
- Furthermore, the human movement could affect the average fluctuation energy a lot at the whole space. The power spectral density was increased by 80% with a moving person (1.0 m/s) as compared with the steady state condition. The turbulent kinetic energy was increased by 93%, and the fluctuation

energy ratio was also increased by 21% with a 1.0 m/s moving speed.

## Acknowledgements

The author wish to acknowledge comments from Juha Jokisalo, Aalto University.

## Authors' contribution

Weixin Zhao conducted all measurements, analysed data and drafted the article. Simo Kilpeläinen and Risto Kosonen supervised the research and measurements; Risto Kosonen reviewed the article and provided comments for revision of the article.

## Declaration of conflicting interests

The author(s) declared no potential conflicts of interest with respect to the research, authorship, and/or publication of this article.

## Funding

The author(s) received no financial support for the research, authorship, and/or publication of this article.

## ORCID iDs

Weixin Zhao  <https://orcid.org/0000-0003-2571-2023>  
Sami Lestinen  <https://orcid.org/0000-0002-8987-3750>

## References

1. Wargoeki P and Wyon DP. Ten questions concerning thermal and indoor air quality effects on the performance of office work and schoolwork. *Build Environ* 2017; 112: 359–366.
2. Haverinen-Shaughnessy U, Shaughnessy RJ, Cole EC, Toyinbo O and Moschandreas DJ. An assessment of indoor environmental quality in schools and its association with health and performance. *Build Environ* 2015; 93: 35–40.
3. Leech JA, Nelson WC, Burnett TR, Aaron S and Raizenne ME. It's about time: a comparison of Canadian and American time-activity patterns. *J Expo Anal Environ Epidemiol* 2002; 12: 427.
4. Bertheussen B, Mustakallio P, Melikov AK and Kosonen R. Performance of chilled beam with radial swirl jet and diffuse ceiling air supply in heating mode. In: *Clima 2013: 11th REHVA world congress & 8th international conference on IAQVEC*, Prague, Czech Republic, June 16–19 2013.
5. Mustakallio P, Bolashikov Z, Kostov K, Melikov A and Kosonen R. Thermal environment in simulated offices with convective and radiant cooling systems under cooling (summer) mode of operation. *Build Environ* 2016; 100: 82–91.
6. Kosonen R, Saarinen P, Koskela H and Hole A. Impact of heat gain location and strength on air flow pattern with a passive chilled beam system. *Energy Build* 2010; 42: 34–42.

7. Koskela H, Hägglblom H, Kosonen R and Ruponen M. Flow pattern and thermal comfort in office environment with active chilled beams. *HVAC&R Res* 2012; 18: 723–736.
8. Lestinen S, Kilpeläinen S, Kosonen R, Jokisalo J and Koskela H. Experimental study on airflow characteristics with asymmetrical heat gain distribution and low-momentum diffuse ceiling ventilation. *Build Environ* 2018; 134: 168–180.
9. Lestinen S, Kilpeläinen S, Kosonen R, Jokisalo J, Koskela H and Melikov AK. Flow characteristics in occupied zone – an experimental study with symmetrically located thermal plumes and low-momentum diffuse ceiling air distribution. *Build Environ* 2018; 128: 77–88.
10. Bertheussen B, Mustakallio P, Kosonen R and Melikov AK. Comparison of the performance of chilled beam with swirl jet and diffuse ceiling air supply: impact of heat gain distribution. In: *Clima 2013: 11th REHVA world congress & 8th international conference on IAQVEC*, Prague, Czech Republic, June 16–19 2013.
11. DeHart RL. Health issues of air travel. *Annu Rev Public Health* 2003; 24: 133–151.
12. Mangili A and Gendreau MA. Transmission of infectious diseases during commercial air travel. *Lancet* 2005; 36: 989–996.
13. Mazumdar S, Poussou SB, Lin CH, Isukupalli SS, Plesniak MW and Chen Q. Impact of scaling and body movement on contaminant transport in airliner cabins. *Atmos Environ* 2011; 45: 6019–6028.
14. Tao Y, Inthavong K, Petersen P, Mohanarangam K, Yang W and Tu J. Vortex structures and wake flow analysis from moving manikin models. *Indoor Built Environ*. Epub ahead of print 5 January 2020. DOI: 1420326X19893013
15. Poussou SB, Mazumdar S, Plesniak MW, Sojka PE and Chen Q. Flow and contaminant transport in an airliner cabin induced by a moving body: model experiments and CFD predictions. *Atmos Environ* 2010; 44: 2830–2839.
16. Mattsson M. Velocity field created by moving objects in rooms. In: *RoomVent 1996: Proceedings of the 5th international conference on air distribution in rooms*, Yokohama, Japan, July 17–19 1996.
17. Mattsson M, Bjørn E, Sandberg M and Nielsen PV. Simulating people moving in displacement ventilated rooms. In: *Proceedings of the 5th international conference on healthy buildings*, Washington DC, USA, September 27–October 3 1997.
18. Matsumoto H. Influence of moving object on air distribution in ventilated rooms. In *RoomVent 2002: Proceedings of the 8th international conference on room air distribution*, Technical University of Denmark (DTU), Lyngby, September 8–11 2002.
19. Matsumoto H, Matsusaki A and Ohba Y. CFD Simulation of air distribution in displacement ventilated rooms with a moving object. In: *Proceedings of Roomvent Congress*. University of Coimbra, Coimbra, Portugal 5–8 September 2004.
20. Feng L. Experimental study on the influence of human motion in displacement ventilation room on air distributions. In: *Healthy Buildings 2019 Asia*, Chengsha, Hunan, October 22–25 2019; paper 1363282.
21. Matsumoto H and Ohba Y. The influence of a moving object on air distribution in displacement ventilated rooms. *J Asian Architect Build Eng* 2004; 3: 71–75.
22. Halvoňová B and Melikov AK. Performance of “ductless” personalized ventilation in conjunction with displacement ventilation: Impact of disturbances due to walking person(s). *Build Environ* 2010; 45: 427–436.
23. Yang B and Sekhar C. Interaction of dynamic indoor environment with moving person and performance of ceiling mounted personalized ventilation system. *Indoor Built Environ* 2014; 23: 920–932.
24. Han Z, Weng W and Huang Q. Numerical and experimental investigation on the dynamic airflow of human movement in a full-scale cabin. *HVAC&R Res* 2014; 20: 444–457.
25. Han ZY, Weng WG, Huang QY, Fu M, Yang J and Luo N. Aerodynamic characteristics of human movement behaviours in full-scale environment: comparison of limbs pendulum and body motion. *Indoor Built Environ* 2015; 24: 87–100.
26. Shih YC, Chiu CC and Wang O. Dynamic airflow simulation within an isolation room. *Build Environ* 2007; 42: 3194–3209.
27. Wu W and Lin Z. An experimental study of the influence of a walking occupant on three air distribution methods. *Build Environ* 2015; 85: 211–219.
28. Cheng Y and Lin Z. Experimental investigation into the interaction between the human body and room airflow and its effect on thermal comfort under stratum ventilation. *Indoor Air* 2016; 26: 274–285.
29. Luo N, Weng W, Xu X and Fu M. Human-walking-induced wake flow – PIV experiments and CFD simulations. *Indoor Built Environ* 2018; 27: 1069–1084.
30. Ren C, Feng Z, Cen D and Cao SJ. Study on the subway environment induced by moving train using Gaussian distributed momentum source theory method. *Indoor Built Environ* 2019; 28: 1083–1091.
31. Cao SJ, Cen D, Zhang W and Feng Z. Study on the impacts of human walking on indoor particles dispersion using momentum theory method. *Build Environ* 2017; 126: 195–206.
32. Wang C, Holmberg S and Sadrizadeh S. Impact of door opening on the risk of surgical site infections in an operating room with mixing ventilation. *Indoor Built Environ* Epub ahead of print 17 November 2019. DOI: 1420326X19888276
33. Vellei M and Le Dréau J. A novel model for evaluating dynamic thermal comfort under demand response events. *Build Environ* 2019; 160: 106215.
34. Lindab. Ventiduct VSR, (2017) *Internet reference*, <https://itsolution.lindab.com/lindabwebproductsdoc/pdf/documentation/comfort/us/technical/vsr.pdf> (2017, accessed 13 November 2017).
35. NT VVS 095. Laboratory fume hoods: performance. *Nordtest*, Espoo, Finland, 1993.
36. ANSI/ASHRAE 55-2010. *Thermal environmental conditions for human occupancy*. Atlanta: American Society of Heating Refrigerating and Air-Conditioning Engineers, 2010.

37. ISO 7726:1998. *Ergonomics of the thermal environment – instruments for measuring physical quantities*. Geneva: The International Organization for Standardization, 1998.
38. ThermaCAM™ P60. The professional thermographer's choice, [www.inspectahire.com/media/brochures/1400090001.pdf](http://www.inspectahire.com/media/brochures/1400090001.pdf). (2017, accessed 13 November 2017).
39. ISO 7726: 1998. *Ergonomics of the thermal environment: instruments for measuring physical quantities*. Geneva: International Organization for Standardization, 1998.
40. Zhang S, Cheng Y, Huan C and Lin Z. Heat removal efficiency based multi-node model for both stratum ventilation and displacement ventilation. *Build Environ* 2018; 143: 24–35.
41. ISO 7730:2005. *Ergonomics of the thermal environment – analytical determination and interpretation of thermal comfort using calculation of the PMV and PPD indices and local thermal comfort criteria*. Geneva: The International Organization for Standardization, 2005.
42. Zhou G, Melikov AK and Fanger PO. Impact of equivalent frequency on the sensation of draught. In: *Roomvent 2002: Proceedings of the 8th International conference on air distribution in rooms*, Copenhagen, Denmark, September 8–11 2002. Lyngby: Technical University of Denmark (DTU); pp.297–300.
43. Zhou G and Melikov AK. Equivalent frequency – a new parameter for description of frequency characteristics of airflow fluctuations. In: *Roomvent 2002: proceedings of the 8th international conference on air distribution in rooms*, Copenhagen, Denmark, September 8–11 2002. Lyngby: Technical University of Denmark (DTU); pp. 357–336.
44. Hanzawa H, Melikov AK and Fanger PO. Airflow characteristics in the occupied zone of ventilated spaces. *ASHRAE Trans* 1987; 93: 3045.
45. Welch P. The use of fast Fourier transform for the estimation of power spectra: a method based on time averaging over short, modified periodograms. *IEEE Trans Audio Electroacoust* 1967; 15: 70–73.
46. CEN 1752:1998. *Ventilation for buildings: design criteria for the indoor environment*. Brussels: Committee of European Standardization, 1998.
47. Melikov AK, Popiolek Z, Silva MCG, Care I and Sefker T. Accuracy limitations for low-velocity measurements and draft assessment in rooms. *HVAC&R Res* 2007; 13: 971–986.
48. Tobin P. PSpice for digital communications engineering. *Synthesis Lect Digital Circuits System* 2007; 2: 1–199.
49. Koopmans LH. *The spectral analysis of time series*. Amsterdam: Elsevier, 1995.
50. Kolmogorov AN. The local structure of turbulence in incompressible viscous fluid for very large Reynolds numbers. In: *The Proceedings of the Royal Society of London*. Series A: Mathematical and Physical Sciences. 1991; 434: 9–13.
51. Melikov AK, Langkilde G and Derbiszewski B. Airflow characteristics in the occupied zone of rooms with displacement ventilation. *ASHRAE Trans* 1990; 96: 555–563.
52. Cheng Y and Lin Z. Experimental study of airflow characteristics of stratum ventilation in a multi-occupant room with comparison to mixing ventilation and displacement ventilation. *Indoor Air* 2015; 25: 662–671.